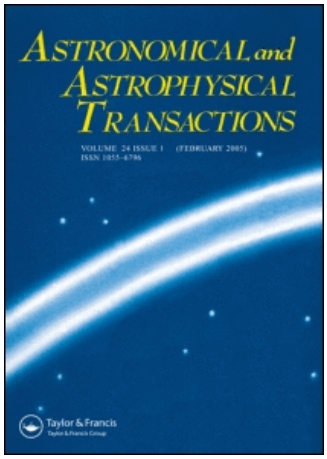

Astronomical & Astrophysical Transactions
The Journal of the Eurasian Astronomical Society
Publication details, including instructions for authors and subscription information:
http://www.informaworld.com/smpp/title~content=t713453505

The spatial anisotropy of flares relative to sunspot groups and vector butterfly diagrams in solar activity cycles nos. 17-19 and 23

V. V. Kasinsky [a]
[a] Irkutsk Institute of transport engineers, Irkutsk, Russia

Online Publication Date: 01 October 2001
To cite this Article: Kasinsky, V. V. (2001) 'The spatial anisotropy of flares relative to sunspot groups and vector butterfly diagrams in solar activity cycles nos. 17-19 and 23', Astronomical & Astrophysical Transactions, 20:3, 551 - 557
To link to this article: DOI: 10.1080/10556790108213598
URL: http://dx.doi.org/10.1080/10556790108213598

Astronomical and Astrophysical Transactions, 2001, Vol. 20, pp. 551–557
Reprints available directly from the publisher
Photocopying permitted by license only

THE SPATIAL ANISOTROPY OF FLARES RELATIVE TO SUNSPOT GROUPS AND VECTOR BUTTERFLY DIAGRAMS IN SOLAR ACTIVITY CYCLES NOS. 17–19 AND 23

V. V. KASINSKY

Irkutsk Institute of transport engineers, 664074, Irkutsk, Russia

(Received October 11, 2000)

Data on the location of flares covering solar cycles Nos. 17–19 were used to construct vector $R(\varphi, t)$ diagrams for the mean position of the flares in the coordinate system of the sunspot's group centre. The $R(\varphi, t)$ diagram reveals a global anisotropy of the flare process relative to the midline of the diagram. The R_φ-shift is always directed towards the central part of the diagram. The longitudinal component ($R\lambda$) has the character of oppositely directed shears relative to the epicentral line of the diagram. The opposite $\pm R_\lambda$-shifts of flares are interpreted as the aberration effect of flares. This implies a velocity C of trigger-like disturbance of flares. It follows that $C = 1$–2 km s^{-1}, which corresponds to the low frequency ($\omega < 6$ min) 'internal gravity waves' of the chromosphere.

KEY WORDS Butterfly diagrams, spatial anisotropy of flares, global trigger of flares

Maunder diagrams of sunspots known as 'butterfly diagrams' (BD) have existed since 1901 and serve as a good illustration of the Spörer law (Gibson, 1973). The structure in a number of flares seen on the BD diagrams (Krivsky and Knoska, 1967) raises a question as to whether the distribution of flares in the coordinate system of related sunspots is isotropic and independent of the position of sunspots. This problem cannot be solved by studying only scalar BDs. It is necessary to study the mutual arrangement of sunspots and flares. In recent publications the anisotropy index of flares $R(\varphi, t)$ on the φ–t diagram was calculated for four solar cycles Nos. 17–20 (Kasinsky, 1981, 1988, 1989). This calls for further confirmation using data on the next solar cycles as it is important for the future flare model (Rust and Bridge, 1975; Gershberg, Mogilevsky, and Obridko, 1987; Syrotasky, 1966). It is the objective of this paper to confirm the vector diagram of flares for the 17–19th and the 23rd solar cycles as well.

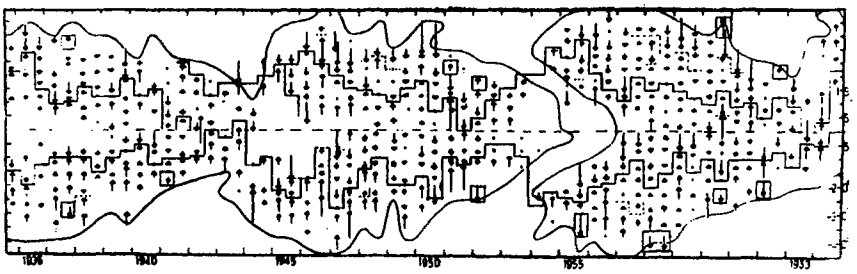

Figure 1 $R(\varphi, t)$-diagram of the R_φ-component of flares in the coordinate system of the sunspot centre constructed for the cycles N 17–19 (1954–1964).

1 LATITUDINAL VECTOR DIAGRAMS OF FLARES IN CYCLES 17–19

Data are taken from the *Quarterly Bulletin on Solar Activity* (1935–1976) (IAU, Zurich, 1935–1976). The coordinates (φ) of over 27000 flares were used in the analysis. The mean position of the flare scattering centre with respect to the sunspot group was calculated using the formula:

$$\langle R_\varphi \rangle = \frac{1}{N} \sum_i \sum_s (\varphi_{is} - \varphi_s), \tag{1}$$

where φ is is the flare's latitude in the s – sunspot, φ_s is the latitude of the sunspot's centre, and N is a total number of flares. The summation in (1) is made over all groups (s) falling within the latitude-time interval $\Delta\varphi \times \Delta t = 5° \times 0.5$ year in this case. The r.m.s. of the mean $\langle R \rangle - \sigma$ should decrease as $(N)^{1/2}$, where N is the number of flares in a sunspot. With the given r.m.s error, in one measurement $s \sim 1$–$2°$, when $N \geq 100$, the error in the displacement $\langle R \rangle$ does not exceed $\pm 0.2°$.

Figure 1 presents the VDF calculated for cycles Nos 17–19 (1935–1964) (Kasinsky, 1988, 1989). The latitude-time resolution on the diagrams spans the range $5° \times 0.5$ year. The step-like line divides each wing of VDF (northern and southern) into near equal parts, with the arrows having opposite directions ($\pm R$), that is equatorial and polar. The VDF was constructed with allowance made for 'weight'. The 'weight' of a vector is the number of flares (N) in the relevant area of the φ–t-diagram according to (1). The scale of the vectors in Figure 1 is magnified 5 times compared with the scale of the latitude axis. The areas of isotropic distribution of flares are determined by the $|R| = 0$ condition (the step-like line). The results show quite clearly that the absolute value of vector $|R|$ increases as the diagram periphery is approached, while the flare vectors consistently point to the diagram centre at which the flare scattering tended to be isotropic, $R \to 0$.

Figure 1 shows that the flare process is anisotropic with respect to the centre of the φ–t-diagram in such a way that their mean positions are systematically displaced to the centre of the diagram. Hence, the spatial characteristics of flare generation in sunspots strongly depend on their position on the diagram. The distribution

of flares becomes homogeneous and isotropic only on the midline of the diagram, $R = 0$. One can see that midlines start at high latitudes and descend towards the equator, following Sporer's law.

If the modulus of R is taken to be the measure of spatial anisotropy of flares in latitude, then the condition $R = 0$ corresponds to the isotropy condition of flares relative to the coordinate system sunspot group centre. Along the geometric line of $R(\varphi, t) = 0$, there is an isotropy of flares in the pole-equator direction in the coordinate system of sunspots. This line on the φ–t-diagram may be defined as the 'epicentre of flaring activity' on the butterfly diagram. Hence the overall tendency of the flare anisotropy has a centripetal character relative to the diagram's center.

2 LONGITUDINAL VECTOR DIAGRAM OF FLARES AND THE ABERRATION EFFECT

The longitudinal component of the mean displacement of flares was calculated using the data on longitude position of flares from the central meridian – λ (cm) according to the *Quarterly Bulletin* (Quarterly Bulletin of Solar Activity. IAU, Zurich, 1935–1976). To reduce λ to the frame of reference tied to a sunspot group rotating on the solar surface, we used the formula of mean differential rotation (Allen, 1955). The flare position with respect to the sunspot's centre is defined by:

$$\Delta\lambda_{is} = \lambda_{is} - \omega(\varphi)[t_{is} - t_s(\text{cmp})], \tag{2}$$

$$\omega(\varphi) = 13.^\circ 38 - 2.^\circ .77 \sin^2 \varphi, \tag{3}$$

where λ_{is} is the central meridian distance of the is-th flare, t_{is} is the flare onset time, t_s is the time of sunspot group passage through the central meridian (cmp), and $\omega(\varphi)$ is the diurnal angular velocity of synodic rotation of sunspots at the latitude φ_s. As was done in formula (1), we take a double average, first over all flares in a given sunspot and, secondly, over all sunspots in a given interval of the φ–t-diagram.

The vector diagram R_λ – component of flares thus calculated – are shown in Figure 2. They are superimposed in the 17th and 18th cycles centred on the maximum epoch. For the sake of illustration, the scale of vectors R_λ is taken to be ten times larger compared with that of the latitude axis. The value of R_λ varies in the range from 0.5° to several degrees. As in the case of vector diagrams for latitudinal displacements (Figure 1), it is possible to draw zero lines $R_\lambda = 0$ which divide the φ–t-diagram into areas with opposite character of the direction of R_λ. As these lines (dashed) cross in the φ-direction, the sign of R_λ changes to the opposite. As is evident in Figure 2, the ($R_\lambda = 0$) – lines drift from high to low latitudes, according to Sporer's law on the whole.

Specifically, below the φ–t-diagram midline the displacements are directed eastward ($R_\lambda < 0$), and above the midline they are directed westward ($R_\lambda > 0$). We will call this type of $\pm R_\lambda(\varphi, t)$ asymmetry the 'normal' type. The opposite type

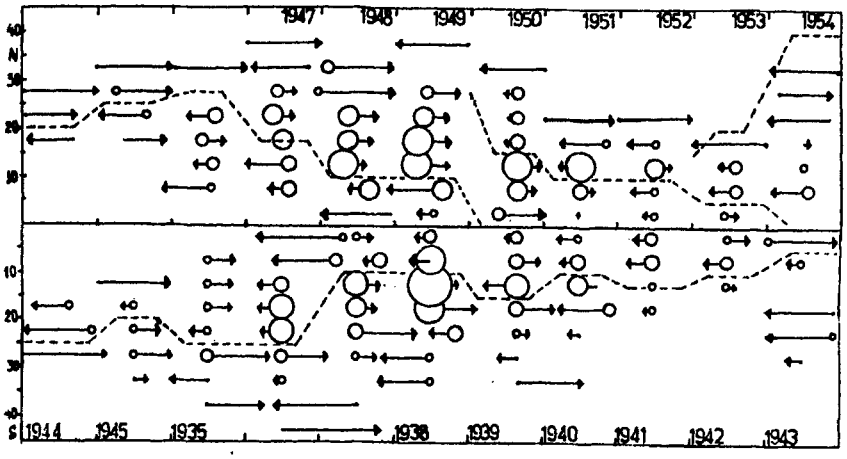

Figure 2 R-vector diagrams for latitudinal displacement of the flare in the 17–18th cycles superimposed by the epoch of maxima. The dashed line represents the zero midline of $R(\varphi, t) = 0$.

of asymmetry occurs more rarely. The normal R_λ asymmetry also shows a tendency for the absolute value of $|R_\lambda|$ to increase with increasing distance from the φ–t-diagram centre.

It is apparent from Figure 2 that the system of E–W-like shifts on the φ–t-diagram has a tendency to persist during the course of an 11-year cycle as the zero midline descends to the solar equator. As in the case of Figure 1 the zero midline ($R_\lambda = 0$) drifts from high to low latitudes, according to Sporer's law. Therefore this midline is to be identified with the drifting sunspot formation 'trajectory' on the φ–t-diagram.

The mean value of R_φ from (1) and the corresponding value of R_λ from (4) forms the components of vector $\boldsymbol{R}(\varphi, t)$ which can be referred to each point on the φ–t-diagram. Therefore this vector butterfly diagram of flares characterizes the magnitude and direction of non-isotropisation of the flare distribution in the sunspots on the φ–t-diagram.

From the previous it necessarily follows that the centre of the vector diagram $\boldsymbol{R}(\varphi, t)$ is a physically significant one. It may serve as a possible source for a global, triggering disturbance with regard to flares. We also assume that this triggering disturbance gives rise to a flare at a point within the group which is reached as a result of the propagation from mid φ_0 latitude of the diagram to a given sunspot latitude φ_s. Because different sunspots belong to different zones of rotation, the high-latitude sunspots will lag behind the disturbance, while those near the equator in which the groups rotate faster will overtake the disturbance. The high-latitude zones will show a positive R_λ, a westward shift of flares, while low-latitude zones will show a negative, eastward shift of flares. Those opposite $\pm R_\lambda$ shifts on the high and low latitudes may be interpreted as the longitudinal aberration effect of flares (Kasinsky, 1994).

It is well known that the aberration of light gives for the angular displacement β of the visual position of a star: $\tan\beta = V/C$, where V is the observer's velocity, and C is the velocity of light. Instead of V, we should substitute the velocity difference of the sunspots due to differential rotation, $V(\varphi) - V(\varphi_0)$, where φ is the flaring sunspot latitude, and φ_0 is the mean latitude on the φ–t-diagram supposed to be a primary source of flare trigger. In our case we have:

$$V(\varphi) - V(\varphi_0) = R_\odot[\omega(\varphi)\cos\varphi - \omega(\varphi_0)\sin\varphi_0], \quad (4)$$

where $R_\odot$ – Sun radius (6.96×10^5 km), $\omega(\varphi)$ given by the calculations. Bearing in mind that $\tan\beta \sim \beta = |R_\lambda|/(\varphi - \varphi_0)$, the determination of C reduces to finding the aberration angle β. We obtain for a mean value of $C \sim 1.1$ km s^{-1} for the first estimate (Kasinsky, 1994).

3 EVIDENCE FOR THE ANISOTROPY OF FLARES AT THE BEGINNING OF THE 23RD CYCLE

The vector diagrams of flares (VDF) in cycles 17–20 (Kasinsky, 1989) are based on the data taken from the *Quarterly Bulletin of Solar Activity* (IAU, Zurich, 1935–1976) The coordinates of sunspots are given when the sunspot passes the central meridian (t–cmp). In order to check the VDF for the epoch of beginning of 23d cycle the data are taken from SWO PRF ('flare list' and 'Region Summary' tables) (Preliminary Report and forecast of SGD-SWO PRF, Bould. Colo. 1999–2000) for a period of 1.5 years (1999–2000). The coordinates (φ, λ) of nearly 1400 flares were used in the analysis. The data differ compared to the *Quarterly Bulletin* in that the position of the sunspot centre is given for each day ($\pm 7d$) of passage across the Sun's disk. Therefore the evolutional changes in the sunspot's position are taken into account automatically. Thus, given formulas (2)–(4) one can define the longitude of a sunspot at the moment of the flare t_i more specifically as

$$\lambda_s = \lambda(D_i) - \omega(D_i)[1 - (t_s/24)], \quad (5)$$

where $\lambda(D_i)$ is the longitude of sunspot for day D_i, $\omega(D_i)$ is the calculated diurnal angular velocity of synodic rotation of sunspots at the latitude φ_s and $t_i/24$ is the flare onset time (max). The technique for calculating the VDF are defined by (1)–(4).

The data processing was done for 33 (690 flares) sunspots in the N-hemisphere and 26 (700 flares) in the S-hemisphere of the Sun. In order to identify more clearly the regular tendency of R-shift we averaged the $R(\varphi, t)$-distribution over two hemispheres. The run of the R_φ and R_λ values, the r.m.s. errors and the accumulated number of flares (column 3) and mean angular velocity of synodic rotation of sunspots (column 2) are shown in Table 1 as a function of mean latitude φ (column 1). In Table 1 the '+' and '−' signs of $\langle\Delta\varphi\rangle$ denote the polar and equatorial directions. While the '+/−' signs of $\langle\Delta\lambda\rangle$ denote respectively the west/east displacements of R.

Table 1.

φ *sunspots*	$\omega(\varphi)°/d$	*N flares*	$\langle\Delta\varphi\rangle$	*r.m.s*	$\langle\Delta\lambda\rangle$	*r.m.s*
30.4	12.55	178	−0.86	±0.24	+1.25	±0.29
20.9	13.08	285	0.46	±0.34	+0.99	±0.83
17.6	13.11	508	+0.11	±0.02	+0.38	±0.33
12.9	13.25	392	+0.32	±0.51	+0.37	±0.51
10.9	13.65	37	−0.33	±0.05	−0.45	±0.05

Estimating by the line slope (column 6) $\beta = 4°$ we have $\tan\beta = 0.07$. Substituting this into (5–6) we obtain for the value of $C \sim 2.3$ km s^{-1}. So we can take 1–2 km s^{-1} as a good estimate for the flare trigger velocity. The type of disturbance may be internal gravity waves in the compressible atmosphere (More, 1964) propagating with subsonic velocities 1–2 km s^{-1}.

4 CONCLUSION

Over 4 solar cycles the flare distribution in the system of sunspots is inhomogeneous (latitude-dependent) as well as anisotropic (a preferred direction). If the generation of flares in a sunspot depended only on internal magnetic factors, this feature of the $R(\varphi, t)$-diagram would be hard to explain. The fact that the flares distinguish between the direction to the centre of diagram and its periphery imposes additional limitations on models of the flare process. Namely the midline of VDF gives rise to a certain constantly acting trigger-like disturbance which, when reaching the sunspots lying on the periphery of the diagram, causes the observed R-shifts. In this case the agent of a disturbance may be associated with some type of magneto-hydrodynamic wave (Gibson, 1973; More, 1964).

According to the principle of relativity in physics, the intrinsic anisotropy of flares $R(\varphi, t)$ may indicate the action of additional forces other than electromagnetic in the sunspots. They may be essential both for the flaring processes as well as for the flare energetics.

In spite of the progress made so far in observation and modelling of solar flares a full-blown theory of flares does not exist. The most well-developed theory is of magnetic annihilation in the current sheets of the corona (Syrovatsky, 1966). However, analysis of the energetics of large flares has shown that at the upper limit of energy (10^{32} erg) and masses (10^{17} g) in the corona there exist no relevant 'accumulators' of energy (Gershberg, Mogilevsky, and Obridko, 1987). Therefore, alternative sources of energy may exist, that is, the so called 'soliton' model (Mogilevsky, 1980). The global trigger was possibly seen in sympathetic flare phenomena in several active regions (Smith H., Smith E.). The type of disturbance must be internal gravity waves or long gravity waves like tsunami as proposed in (Kasinsky and Krat, 1973). One prediction of the new flare model is that a short-lived population of sunspots

(satellites) serves as a trigger for flares. The short-lived population of sunspots is most probably associated with the emergence of new magnetic flux (Rust and Bridge, 1975). Satellite sunspots as a local trigger do not exclude a possible global trigger.

In conclusion, the centripetal character of the R-anisotropy of the flares on the φ–t-diagrams may be understood in terms of the global triggering scenario of flares. The global-scale excitation of flares by wave-like disturbances, generated in the centre of φ–t-diagram by the constant emergence of new short lived sunspots can explain the main features of the $R(\varphi, t)$-diagrams.

References

Allen, C. W. (1955) *Astrophysical Quantities*, Lon., Athlon Press, 304p.

Gershberg, R. E., Mogilevsky, E. I., and Obridko, V. N. (1987) *Kinematics and Physics of Space Bodies* **3**, No.5, 3 (in Russian).

Gibson, E. G. (1973), *The Quiet Sun*, NASA, Washington. D.C., 330 p.

Kasinsky, V. V. (1981) *Phys. Solariterr. Potsdam* **17**, 37.

Kasinsky, V. V. (1988) *Issled. po Geomagnetizm. Aeronomii i Fizike Solntsa*, Moscow, Nauka, v. 79, p. 25.

Kasinsky, V. V. (1989) In: R.A. Gulyaev (ed.) *Atmospere of the Sun, Interplanetary Space, and Planetary Atmosperes*, IZMIRAN Press, Moscow, p. 116.

Kasinsky, V. V. (1994) *Issled. po Geomagnetizm. Aeronomii i Fizike Solntsa*, Novosibirsk, Nauka, v. 102, p. 152.

Kasinsky, V. V. (1999) *Astron. Astrophys. Trans.* **17**, 341.

Kasinsky, V. V. and Krat, V. A. (1973) *Solar Physics* **213**, 219.

Krivsky, L. and Knoska, S. (1967) *Bull. Astron. Inst. Czech.* **18**, No. 6, 325.

More, D. W. (1964) *Astrophys. J.* **131**, 78.

Mogilevsky, E. I. (1980) *Physics of Solar Activity*, Moscow, Nauka, p. 3.

Preliminary Report and forecast of SGD-SWO PRF, Bould. Colo. 1999–2000.

Quarterly Bulletin of Solar Activity, IAU, Zurich, 1935–1976.

Rust, D. M., Bridge, C. A. (1975) *Solar Physics* **43**, 129.

Smith, H., Smith, E., *Solar flares*, Macmillan comp., New York-London, 426 p.

Syrovatsky (1966) *Astron. J.* **43**, 129.